PFC/RR-85-19

DOE/ET/51013-159
UC20,a,b,d,g

An Axisymmetric Pumping Scheme for the Thermal Barrier in a Tandem Mirror

Xing Zhong Li

September 1985

Plasma Fusion Center
Massachusetts Institute of Technology
Cambridge, Massachusetts 02139 USA

Permanent address: Modern Physics Institute, Department of Physics
Tsinghua University, Beijing, China

Abstract

An axisymmetric pumping scheme is proposed to pump the particles that trap in a thermal barrier without invoking the neutral beam or geodesic curvature. In this scheme a magnetic scraper is moved uni-directionally on the barrier peak to push the barely trapped particles into the central cell. We utilize a potential jump that forms at the peak field for sufficiently strong pumping. The non-collisional catching effect has to be limited by setting an upper limit on the scraping frequency of the magnetic bump. On the other hand, the dynamic stability of the pumping scheme sets a lower limit on the scraping frequency. Using the variational method, we are able to estimate the window between these two limits, which seems feasible for the Tara reactor parameter set. A primary calculation shows that the magnetic bump, $\frac{\Delta B}{B}$, is about 10^{-4} and the scraping frequency, ν_{sc}, is about $10^{+5}sec^{-1}$, which are similar to the parameters required for those for drift pumping.

An Axisymmetric Pumping Scheme for the Thermal Barrier in a Tandem Mirror

It has been shown that the performance of a tandem mirror[1] can be importantly enhanced by the use of a "thermal barrier."[2] In this situation a potential depression is interposed between the central cell and plug to thermally isolate the respective electron species. Maintenance of the potential depression depends critically on the ability to purge the barrier of thermal ions that tend to trap there, and which would otherwise cause a decrease of the depth of the potential depression. The purging of trapped ions has been termed barrier pumping.

There have been two kinds of pumping schemes. One is the neutral beam pumping,[3] which uses the energetic neutral beam to neutralize the trapped particles and purge them out the confinement system. This scheme is based upon the charge exchange process, which is not very efficient at reactor regime. Therefore, a drift pumping[4] scheme was proposed to purge the trapped ions in the tranverse direction. This drift-pumping scheme is based on the geodesic curvature of the magnetic field line, which induces the drift motion across the flux surface. However, when the consideration of the transport makes axisymmetric configuration more attractive, an axisymmetric pumping scheme is more desirable. In the present paper we are proposing a pumping scheme which does not depend on geodesic curvature or charge exchange process.

From the thermodynamics point of view, the pumping process is to reverse an irreversible process, the trapping process. We must do some work on the diffusing medium in order to reverse a diffusion process. Compressing the dilute trapped particles and sending them back to the central cell directly is an economical way to handle this process. During the trapping process, the orderly energy is turned into random energy due to collisions. In order to reduce the necessary work to reverse this process, it is better to pump back the barely trapped particles, since the less collisions they experience, the less the necessary work is required to reverse this process.

Fig. 1a and b show the trajectories of the barely trapped particles in a thermal barrier and their population in velocity space, respectively. Most of the barely trapped particles are concentrated at the vicinity of the vertex of the passing-trapped separatrix. If we shift the barrier peak to the left (Fig.1c), the space occupied by these barely trapped particles will increase; therefore, their density will decrease, which is equivalent to a kind of pumping. In order to keep this process continuing, we have to reestablish the barrier peak at the right edge and move it towards the left again.

Fig. 2a shows schematically an axisymmetric scheme to scrape the barely trapped particles by a moving magnetic field. The solid line shows the magnetic field profile. The central cell is located to the left of the barrier peak. If the location of the magnetic field maxima is able to move (from the right to left) it creates a depleted region at its right, where the density in velocity space is different from before. (The passing particles occupy only the hatched region). The depleted region may be filled by the barely trapped particles in the thermal barrier region due to the flow, by the locally trapped particles in the barrier peak region due to collisions, or some non-collisional effect.

Fig. 2b shows the sequence of the moving peak, which appears first at the right edge of the barrier peak and disappears when it moves to the left edge of the barrier peak. The new peak appears again at the right edge before the old one disappears. The necessary moving frequency, ν_{sc} and the amplitude, $\frac{\Delta B}{B_m}$, of the moving peak are two important parameters for this scheme. There are two questions which should be answered before it becomes a realistic pumping scheme. The first question is whether there is actually an evacuated region at the right of the barrier peak? If some trapping processes grow and fill this evacuated region before the barely trapped particles in the thermal barrier flow into this evacuated region, then this pumping scheme may not be effective. The second question is whether this is a dynamically stable pumping scheme? Since only a portion of the trapped particles is pumped by this pumping scheme, one may worry about the dynamic stability of this pumping process. The answers to these two questions are affirmative, provided that these two pumping parameters (ν_{sc} and $\frac{\Delta B}{B_m}$) are in the effective range. In fact, the amplitude of the moving peak ($\Delta B/B_m$) is determined by the engineering limit, but the effectiveness sets an upper limit for scraping frequency, ν_{sc}, and the requirement of stability sets a lower limit for the scraping frequency.

We start from the discussion of the upper limit for scraping frequency. As pointed by D.E. Baldwin[5], when a magnetic well or an electro-static well is developing, a collisionless trapping can occur so that this region is not totally depleted of trapped particles. A typical example is shown in the Fig. 3. At t = 0, there is no electrostatic potential at all, all particles in velocity space are passing particles. At $t = \Delta t$, an electrostatic potential well is imposed in the length of L_b.

The particles with small parallel velocity would be trapped by this developing potential since the particle will feel less acceleration as it enters the well than when it tries to leave the other edge of the well. Qualitatively, this trapped region can be written as

$$v_{||} < \left(\frac{L_b}{\Delta t} \left(\frac{2\Delta\phi}{m} \right)^{1/2} \right)^{1/2} \tag{1}$$

If $\left(\frac{L_b}{\Delta t} \right) \ll \left(\frac{2\Delta\phi}{m} \right)^{1/2}$, then the boundary is at

$$v_{||} \ll \left(\frac{2\Delta\phi}{m} \right)^{1/2} \tag{2}$$

Therefore, only a small portion of the particles are trapped by the non-collisional process. We may call it "catching process," since the developing potential is catching up the slow moving particles before they run out from the potential well. Therefore, to avoid a large "catching" rate we must limit the rate of formation of the potential depression.

The same is true for a developing magnetic well. In Fig. 4, at t = 0, there is a uniform magnetic field; at $t = \Delta t$, a magnetic well (ΔB) is developing in the length of L_b. The particles with small parallel velocity would be trapped by this developing magnetic well also, since the particles may feel less acceleration at one edge of the well, and feel more deceleration at another edge of the well. Qualitatively, this trapped region can be written as

$$v_{||} < \left(\frac{L_b}{\Delta t} \; v_{\perp} \left(\frac{\Delta B}{B_m} \right)^{1/2} \right)^{1/2} \tag{3}$$

If

$$\left(\frac{L_b}{\Delta t} \right) \ll v_{\perp} \left(\frac{\Delta B}{B_m} \right)^{1/2} \tag{4}$$

then the boundary is at

$$v_{||} \ll v_{\perp}\left(\frac{\Delta B}{B_m}\right)^{1/2} \tag{5}$$

Therefore, only a small portion of the particles are trapped by the catching process.

In a word, the scraping process can not be very fast, ie. $\left(\frac{L_b}{\Delta t}\right)$ can not be too large in order to evacuate the velocity space. This turns out to be the upper limit of the scraping frequency ν_{sc}, since $\nu_{sc} \sim \frac{1}{\Delta t}$.

One may notice that the magnitude of $\left(\frac{\Delta B}{B_m}\right)$ is limited by the engineering design. It is the order of $10^{-3} \sim 10^{-4}$. Therefore, only a thin layer on the passing-trapped boundary will be pumped by scraping region in the scheme discussed above. However, the most important region to pump is the vertex of the passing-trapped boundary.[6] Fortunately, it has been shown that a potential sheath can form at the magnetic field maxima[7], which can increase greatly the size of the pumped region. Sheath formation requires that the trapped particle population not be too large. Typically the potential jump will disappear when the pumping factor $g_b \leq 1.09$[8]. (Here, g_b is defined as the ratio of the total density to the passing particle density). Since the catching effect may increase the trapping factor, g_b, it can diminish the potential jump. In the Appendix A, we have a rough estimate of the upper limit of the scraping frequency, below which the potential jump exists. For the time being, we take this scraping frequency as an order of 10^4- $10^5 sec^{-1}$, and discuss the stability of this pumping scheme.

Now we discuss the lower limit for scraping frequency, below which this scraping pumping scheme may not be dynamically stable. When only a portion of the trapped particles are pumped, there is always a stability problem. Since the trapped particles in the unpumped region may contribute to the collisional diffusion process but not the pumping process, it is difficult to purge these unpumped regions. Usually, these trapped particles are purged indirectly by the stronger pumping in the pumped region. If this pump is not strong enough, the accumulation of the particles in the unpumped region may increase the trapping rate further and diminish the barrier eventually. However, either the numerical solution of the Fokker-Planck equation[9] or the analytical calculation of the low energy beam pumping[10] has shown that it is still possible to reach a stable thermal barrier, as long as the pumping is strong enough. This magnetic scraper pumping scheme pumps the vicinity of the passing-trapped boundary only; therefore, it is necessary to analyze its stability.

In general, we know that the trapping current is proportional to the square root of the pumping factor,[6]

$$J_{trap} \propto \sqrt{g_b} \tag{6}$$

because the diffusion coefficient is proportional to g_b, and the gradient of the distribution function is inversely proportional to $\sqrt{g_b}$. On the other hand the pumping current is proportional to $(g_b - 1)$

$$J_{pump} \propto (g_b - 1) \tag{7}$$

because it is proportional to the number of the trapped particles. Fig. 5 shows the curves for J_{trap} and J_{pump} vs. g_b. The intersection of these two curves will give the equilibrium value of g_b. It is evident that the first intersection must be the stable equilibrium, since the derivatives near the intersection satisfy the condition

$$\frac{dJ_{pump}}{dg_b} > \frac{dJ_{trap}}{dg_b} \tag{8}$$

Any deviation from the equilibrium will decay automaticaly. However, if all of the trapped particles are not pumped out, we have[10]

$$\frac{dJ_{pump}}{dg_b} \propto (g_b - 1) \frac{1}{1 + \frac{n_{tH}}{n_{tL}}} \tag{9}$$

Here, the same notations as those in Ref. [10] are used. Ratio $\frac{n_{tH}}{n_{tL}}$ shows the ratio of trapped particle density in the unpumped region to that in the pumped region. This ratio may increase with g_b, and the curve $J_{pump}(g_b)$ is no longer a straight line. Fig. 6 shows the two different cases by the dotted line. For the curve 1, there are two intersections, one stable and the other unstable $\left(\frac{dJ_{pump}}{dg_b} < \frac{dJ_{trap}}{dg_b}\right)$. The curve 2 has no solution at all, because the pump is too weak. All these different cases have been seen in the numerical solution of the Fokker-Planck equation already.

In the following, we use the two group-single sphere model[6] to evaluate the currents J_{pump} and J_{trap} for a typical tandem mirror reactor parameter set: the barrier mirror ratio $R_b = 6$, the barrier potential depth $\phi_b = 3\ T_p$, the temperature of the passing particles $T_p = 24$ KeV, the passing particle density $n_p = 5 \times 10^{13} cm^{-3}$. Having defined the dimensionless currents

$$\hat{J}_{trap} \equiv \frac{J_{trap}}{\nu_L n_p} \tag{10}$$

and

$$\hat{J}_{pump} \equiv \frac{J_{pump}}{\nu_L n_p} , \tag{11}$$

we have

$$\hat{J}_{trap} \approx 10.9 \left(\frac{g_b}{\nu_L}\right)^{1/2} \tag{12}$$

and $$\hat{J}_{pump} \approx \frac{(g_b - 1)}{1 + c_1(1 + \nu_L c_2/g_b)^{-1}} \tag{13}$$

Here, ν_L is the effective pumping rate in the pumped region. c_1 and c_2 are two constants (see Appendix B)

$$c_1 \approx \frac{3\sqrt{\pi}}{4} \left(\frac{T_p}{\phi_1 R_b}\right)^{3/2} \tag{14}$$

$$c_2 \approx \frac{3\sqrt{\pi}}{20} \frac{1}{\nu_p} \left(\frac{1}{R_b}\right)^{1/2} \frac{\phi_1}{T_p} \qquad (15)$$

Here, ν_p is the collision frequency

$$\nu_p = \frac{\Gamma n_p}{\nu_T^3} \qquad (16)$$

where $\Gamma = \frac{4\pi e^4 \ln\Lambda}{m^2}$ with m and e the mass and the charge of the ion, $\ln\Lambda$ the coulomb logarithum; $v_T = \sqrt{\frac{2T_p}{m}}$ the thermal velocity. ϕ_1, is defined[10] as

$$\phi_1 = 2\phi_b - \phi_L - 2\sqrt{\phi_b(\phi_b - \phi_L)} \qquad (17)$$

Here, ϕ_L is the potential jump in the vicinity of the barrier peak. The existence of this potential jump will greatly enlarge the region in velocity space that is being pumped, as is evident from Eq. (13).

Fig. 7 shows the curves for J_{trap} and J_{pump} vs. g_b. It is evident that the effective pumping rate ν_L has to be greater than 10^3 sec^{-1} in order to have a reasonable solution (we notice that the two group - single sphere model is tested only for $1.5 \lesssim g_b \lesssim 5$). It is a stable solution.

Finally, we want to ask how much scraping frequency is necessary to reach this necessary effective pumping rate. Looking at the barrier peak region of Fig. 2b, we can see that the region that is pumped by the moving peak is that in the hatched region.* Therefore, the scraping current is

$$J_{sc} = n_c \sqrt{\frac{\Delta B}{B_m}}\, \nu_{sc} \cdot L_{sc} \cdot \pi r_{sc}^2 \tag{18}$$

Here n_c is the density at the barrier peak region which is about the central cell density. L_{sc} and r_{sc} are the length and the radius of the scraping flux tube. ν_{sc} is the scraping frequency. On the other hand, assuming a thermal barrier length, L_b, and radius, r_b, we have the total pumping current.

$$J_{pump} = \nu_L\, n_p \frac{(g_b - 1)}{1 + \frac{n_{tH}}{n_{tL}}} L_b \cdot \pi r_b^2 \tag{19}$$

Since $\left(\frac{r_b}{r_{sc}}\right)^2 = R_b$, $\frac{n_c}{n_p} \approx R_b \left(\frac{\pi(\phi_b + T_p)}{T_p}\right)^{1/2}$, and

$$\frac{(g_b - 1)}{1 + \frac{n_{tH}}{n_{tL}}} = 10.9 \left(\frac{g_b}{\nu_L}\right)^{1/2}$$, we have

*In fact, if we consider the electrostatic potential, the population which is pushed out by the moving peak is greater; then, the necessary scraping frequency is lower. Hence, the window for scraping frequency would be greater.

$$\nu_{sc}\sqrt{\frac{\Delta B}{B_m}} = \frac{1}{R_b}\left(\frac{T_p}{\pi(\phi_b + T_p)}\right)^{1/2} \cdot \frac{L_b}{L_{sc}} \cdot R_b \cdot \nu_L \cdot 10.9\left(\frac{g_b}{\nu_L}\right)^{1/2}$$

$$= \sqrt{\frac{T_p}{\pi(\phi_b + T_p)}} \cdot \frac{L_b}{L_{sc}} \cdot (\nu_L)^{1/2} \cdot 10.9 \cdot (g_b)^{1/2} \qquad (20)$$

Assuming $\frac{L_b}{L_{sc}} \approx 2$, $\nu_L = 5000\ \text{sec}^{-1}$, and $g_b \approx 5$, we have

$$\nu_{sc}\sqrt{\frac{\Delta B}{B_m}} \approx \sqrt{\frac{1}{\pi(3+1)}} \cdot 2 \cdot (5000)^{1/2} \cdot 10.9 \cdot \sqrt{5}$$

$$= 9.73 \times 10^2\ \text{sec}^{-1} \qquad (21)$$

If $\frac{\Delta B}{B_m} \sim 10^{-4}$, then $\nu_{sc} \sim 9.73 \times 10^4\ \text{sec}^{-1}$. This scraping frequency is enough to create an effective pumping rate of $5 \times 10^3\ \text{sec}^{-1}$, and it is in the reasonable engineering limit. Compared with the upper limit in the Appendix A ($\nu_{sc} < 5 \times 10^5\ \text{sec}^{-1}$) it is well below the necessary value to ensure an electrostatic potential jump.

As a conclusion, we can see that for $\frac{\Delta B}{B_m} \sim 10^{-4}$ and $\nu_{sc} \sim 1 \times 10^5$ sec^{-1}, this magnetic scraper pumping scheme is effective and stable for a tandem mirror reactor. It is axisymmetric such that no transport problem is introduced. There is no requirement for neutral beams and therefore, no neutral gas problem. Additionally, it has no effect on passing particles and hence, the energy efficiency is high. Consequently, we may expect a better Q value reactor (Q is defined as the fusion power over injected power).

We will not discuss here the engineering design for a magnetic scraper pumping system. But the engineering design for a drift pumping scheme[13] is, however, a good reference. The values for $\frac{\Delta B}{B_m}$ and ν_{sc} are in the same range as those for drift pumping. We conclude that it is possible to design an axisymmetric magnetic scraper pumping system.

Appendix A.

The Upper Limit of Scraping Frequency

Starting from R. Cohen's[8] result, we would like to estimate the allowable thickness for the catching effect layer (the hatched region in fig. 8).

Assuming that the catching effect of the electrostatic and the magnetic well has filled a region in velocity space

$$v_{||} < v_c \tag{A-1}$$

at the shoulder of the barrier peak, Fig. 8 shows the diagram for velocity space at the $R_b = 3$, $\phi_b \sim 2.2$ point. The values of v_a, v_c, v_b, determine the boundaries for catching effect layer and passing particle region such that

$$\frac{1}{2} m{v_b}^2 = \phi_b \tag{A-2}$$

$$\frac{1}{2} m{v_b}^2 - \frac{1}{2} m{v_a}^2 = \Delta\phi \tag{A-3}$$

$$v_c = \frac{L_b}{v_c} \frac{1}{\Delta t} \left(\frac{2}{m} \Delta\phi \right)^{1/2} \tag{A-4}$$

Here, $\Delta\phi$ is the potential jump at the shoulder of the barrier peak; L_b is the length of the barrier peak. The passing particle density at the point (R_b, ϕ_b) is

$$n_p = n_c \; H \; (R_b, \frac{\phi_b}{T_p}) \tag{A-5}$$

Here, n_c the central cell density, T_p the temperature of the passing particle density.

$$H \; (R_b, \frac{\phi_b}{T_p}) \approx \frac{1}{R_b} \left(\frac{1}{\pi \; (1 + \frac{\phi_b}{T_p})} \right)^{1/2} \qquad \begin{matrix} (\text{for } R_b > 1) \\ \phi_b > T_p \end{matrix} \tag{A-6}$$

Assuming a maxwellian distribution function in the catching effect layer, we have the trapped particle density

$$n_t \approx n_c H \left(R_b, \frac{\phi_b - \Delta\phi}{T_p} \right) - n_c H \left(R_b, \frac{\phi_b - \Delta\phi + \frac{1}{2} m v_c^{\,2}}{T_p} \right) \tag{A-7}$$

Hence, the pumping factor at (R_b, ϕ_b) point is

$$g_b = \frac{n_p + n_t}{n_p} = 1 + \frac{1}{2} \frac{\frac{1}{2} mv_c^2}{T_p} \qquad \text{(A-8)}$$

R. Cohen found a critical value of $g_b < 1.09$ for electrostatic potential jump $\Delta\phi$. So we have an estimate for $\frac{1}{2} mv_c^2$

$$\frac{\frac{1}{2} mv_c^2}{T_p} = 0.18 \qquad \text{(A-9)}$$

It is noticed that this ratio is approximately independent of R_b, $\frac{\phi_b}{T_p}$ and $\frac{\Delta\phi}{T_p}$. Now we can use this value to calculate the $\frac{\Delta\phi}{T_p}$ self-consistently. At the shoulder of the barrier peak, we have electrical neutrality so that

$$\exp\left(-\frac{\Delta\phi}{T_p}\right) = H\left(1 + \frac{\Delta B}{B_m}, \frac{\Delta\phi}{T_p}\right) + \left[1 - H\left(1, \frac{\frac{1}{2} mv_c^2}{T_p}\right)\right]$$

$$= \exp\left(\frac{\Delta\phi}{T_p}\right) \text{erfc}\left(\sqrt{\frac{\Delta\phi}{T_p}}\right) + \left[1 - e^{0.18} \text{erfc}\left(\sqrt{0.18}\right)\right] \qquad \text{(A-10)}$$

Using the approximate formula[12]

$$e^{\Delta\phi}\text{erfc}\left(\sqrt{\Delta\phi}\right) \approx \frac{0.348}{1 + 0.470\sqrt{\Delta\phi}} \tag{A-11}$$

we have the solution for $\frac{\Delta\phi}{T_p} \approx 0.388$. Since we have obtained the value for v_c and $\frac{\Delta\phi}{T_p}$, we can calculate

$$\frac{L_b}{\Delta t} = \frac{v_c^2}{\left(\frac{2}{m}\,\Delta\phi\right)^{1/2}} = \frac{\frac{1}{2}\,mv_c^2/T_p}{\sqrt{\frac{m}{2T_p}}\left(\frac{\Delta\phi}{T_p}\right)^{1/2}}$$

$$\frac{L_b}{\Delta t}\left(\frac{m}{2T_p}\right)^{1/2} = \frac{1}{2}\;\frac{mv_c^2}{T_p}\left(\frac{T_p}{\Delta\phi}\right)^{1/2} = \frac{0.18}{\sqrt{0.388}}$$

$$\frac{\frac{1}{2}\,m\left(\frac{L_b}{\Delta t}\right)^2}{T_p} = 0.0835$$

$$\frac{L_b}{\Delta t} = 0.29\;v_t$$

$$\nu_{sc} \sim \frac{1}{\Delta t} \sim 0.29 \frac{v_t}{L_b} \sim 0.29 \times \frac{\sqrt{2.4 \times 10^8}}{10^2} \sim 0.45 \times 10^6 \text{ sec}^{-1} \qquad \text{(A-12)}$$

Therefore, the limiting value of g_b from Ref. [8], $g_b = 1.09$, gives an upper limit for scraping frequency of $\nu_{sc} \sim 5 \times 10^5$ sec^{-1}. A higher scraping frequency may cause more catching effect and would diminish the potential jump. The scraping frequency estimated for a reactor parameter is about 10^5 sec^{-1} which is well below this upper limit. So there must be an electrostatic potential jump, which assures the effectiveness of the magnetic scraper pumping scheme.

Appendix B

The Two Group - Single Sphere Model for J_{trap} and J_{pump}

Using the formula (5.10) in the Ref. [6], we have

$$J_{trap} = 2\sqrt{p(o)q_o(0)}$$

$$= 2\sqrt{\nu_L^2 \quad n_p \frac{n_b}{2} \quad \frac{2}{3\pi} \cdot \frac{\nu_c}{\nu_L} \cdot \frac{n_c}{n_p} \cdot \frac{1}{\sqrt{\pi}} \quad \frac{1}{\sqrt{R_b}}}^{\,3} \qquad \text{(B-1)}$$

$$\hat{J}_{trap} = \frac{J_{trap}}{\nu_L \; n_p}$$

$$\approx 2 \; (g_b)^{1/2} \left(\left(\frac{R_b}{\pi} \right)^{1/2} \cdot \frac{1}{3} \cdot \frac{\nu_p}{\nu_L} \left(1 + \frac{\phi_b}{T_p} \right) \right)^{1/2} \qquad \text{(B-2)}$$

For the Tara reactor, $\frac{\phi_b}{T_p} = 3$, $\nu_p = 16.1 \text{ sec}^{-1}$, $R_b = 6$,

$$\hat{J}_{trap} = 10.9 \left(\frac{g_b}{\nu_L} \right)^{1/2} \qquad \text{(B-3)}$$

Using the formulas (1), (6), and (23) of Ref. [10], we have

$$\hat{J}_{pump} \equiv \frac{J_{trap}}{\nu_L \; n_p}$$

$$= \frac{(g_b - 1)}{1 + \frac{n_{tH}}{n_{tL}}} \qquad \text{(B-4)}$$

and

$$\frac{n_{tH}}{n_{tL}} = \frac{C_1}{1 + \frac{\nu_L}{g_b} C_2} \qquad \text{(B-5)}$$

Considering that the temperature T_p in formulas (24) and (25) of Ref. [10] should be the effective temperature (T_p/R_b), we have

$$C_1 = \frac{3}{2}\left(\frac{T_p}{R_b \phi_1}\right)^{3/2} \left\{ \Gamma\left(\frac{3}{2}, \frac{\phi_1 R_b}{T_p}\right) - \Gamma\left(\frac{3}{2}, \frac{R_b \phi_b}{T_p}\right) \right\} \qquad \text{(B-6)}$$

$$C_2 = \frac{3}{20} \sqrt{\pi} \cdot \frac{1}{\nu_p R_b^{3/2}} \cdot \frac{R_b \phi_1}{T_p} \qquad \text{(B-7)}$$

Since $\frac{R_b \phi_b}{T_p} >> 1$, and $\frac{R_b \phi_1}{T_p} << 1$, we have

$$\Gamma \left(\frac{3}{2} , \frac{R_b \phi_1}{T_p} \right) \sim \frac{\sqrt{\pi}}{2} , \tag{B-8}$$

$$\Gamma \left(\frac{3}{2} , \frac{R_b \phi_b}{T_p} \right) \sim 0. \tag{B-9}$$

Therefore,

$$C_1 = \frac{3\sqrt{\pi}}{4} \left(\frac{T_p}{R_b \phi_1} \right)^{3/2} \tag{B-10}$$

$$C_2 = \frac{3}{20} \sqrt{\pi} \frac{1}{\nu_p} \left(\frac{1}{R_b} \right)^{1/2} \frac{\phi_1}{T_p} \tag{B-11}$$

Acknowledgements

Many thanks to Drs. Kesner and Baldwin for their helpful discussion. This work is supported by D.O.E. Contract No. AC02-78ET-51013.

Figure Captions

Fig. 1 a) The trajectory of barely trapped particles in a thermal barrier.

b) The population of the barely trapped particles in velocity space.

c) Moving peak to expand the volume occupied by the barely trapped particles.

Fig. 2 a) A schematic of the axisymmetric pumping scheme.

b) A sequence of the moving peaks.

Fig. 3 Catching effect in a developing "electrostatic potential well."

Fig. 4 Catching effect in a developing "magnetic potential well."

Fig. 5 Dynamically stable solution $\left(\frac{dJ_{pump}}{dg_b} > \frac{dJ_{trap}}{dg_b}\right)$.

Fig. 6 Dynamically stable and unstable solutions.

Fig. 7 Diagram for $\hat{J}_{trap}$ vs. g_b and $\hat{J}_{pump}$ vs. g_b.

Fig. 8 The sheath formation condition.

References

[1] T.K. Fowler and B.G. Logan, Comments on Plasma Physics and Controlled Fusion **2** 167 (1977). G.I. Dimov, $\bar{V}$.$\bar{V}$. Zakaydakov, M. Ye. Kisinevskiy, Fizika Plasmy **2** 597 (1976).

[2] D.E. Baldwin, B.G. Logan, Phys. Rev. Letters, **43** (1979) 1318.

[3] G.A. Calson et.al., "Tandem Mirror Reactor with Thermal Barriers" UCRL - 52836, 123 (1979).

[4] D.E. Baldwin, Bulletin Am. Phys. Soc. Vol. 26, P. 1021, 1981.

[5] D.E. Baldwin, private communication (1985).

[6] X.Z. Li and G.A. Emmert, Nucl. Fusion **24** (1984) 359. X.Z. Li, Docotoral Thesis "A Variational Calculation of the Trapping Current in a Thermal Barrier," Univ. of Wisconsin, 1983.

X.Z. Li and G.A. Emmert (Submitted to Chinese Journal "Scientia Sinica" with English version.)

[7] J. Kesner, G. Knorr and D.R. Nicholson, Nucl. Fusion 21 (1981) 1265.
J. Kesner UWFDM-348 (1980).

[8] R. H. Cohen, Nucl. Fusion 21 (1981) 209.

[9] R.S. Devoto, Nucl. Technology/Fusion 3 (1983) 304.

[10] X.Z. Li, and J. Kesner, Nucl. Fusion 25 (1985), 425.

[11] Sivukhin, D.V.," Coulomb Collision in a Fully Ionized Plasma" in Review of Plasma Physics, edited by Acad., Leontovich M.A., Vol. 4, p. 93 (1966).

[12] M. Abramowitz and I.A. Stegun, "Handbook of Mathematical Functions with Formulas, Graphs, and Mathematical Tables." p. 253 (1972).

[13] B.G. Logan, and W.S. Neef, "A Drift-Pump Coil Design for a Tandem Mirror Reactor", UCRL-89521 (1983).

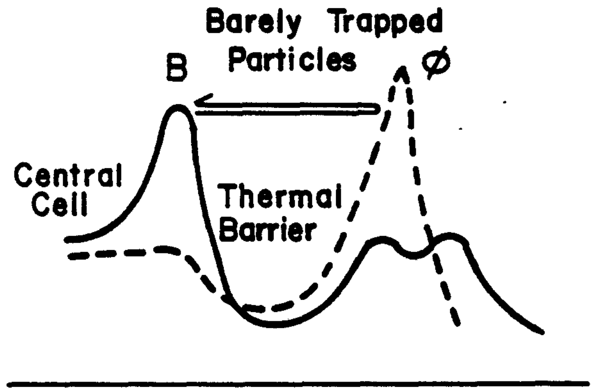

FIG. 1.a.

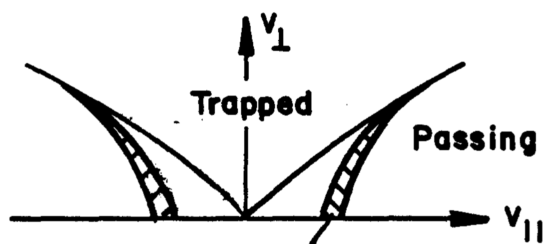

FIG. 1.b.

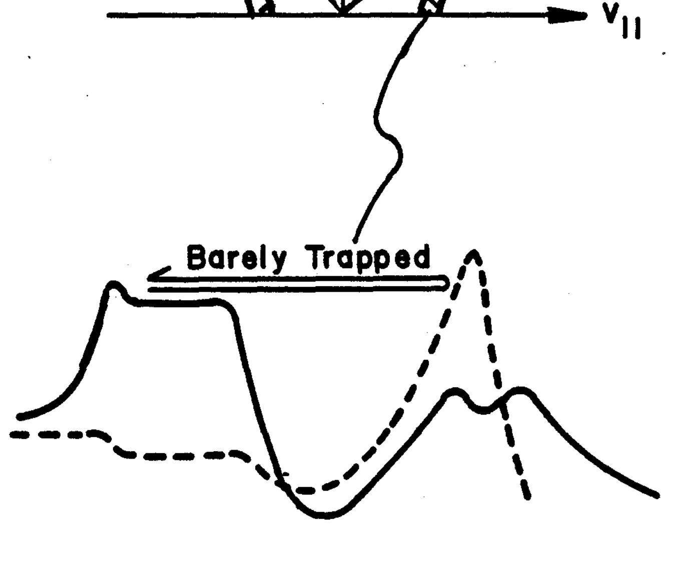

FIG. 1.c.

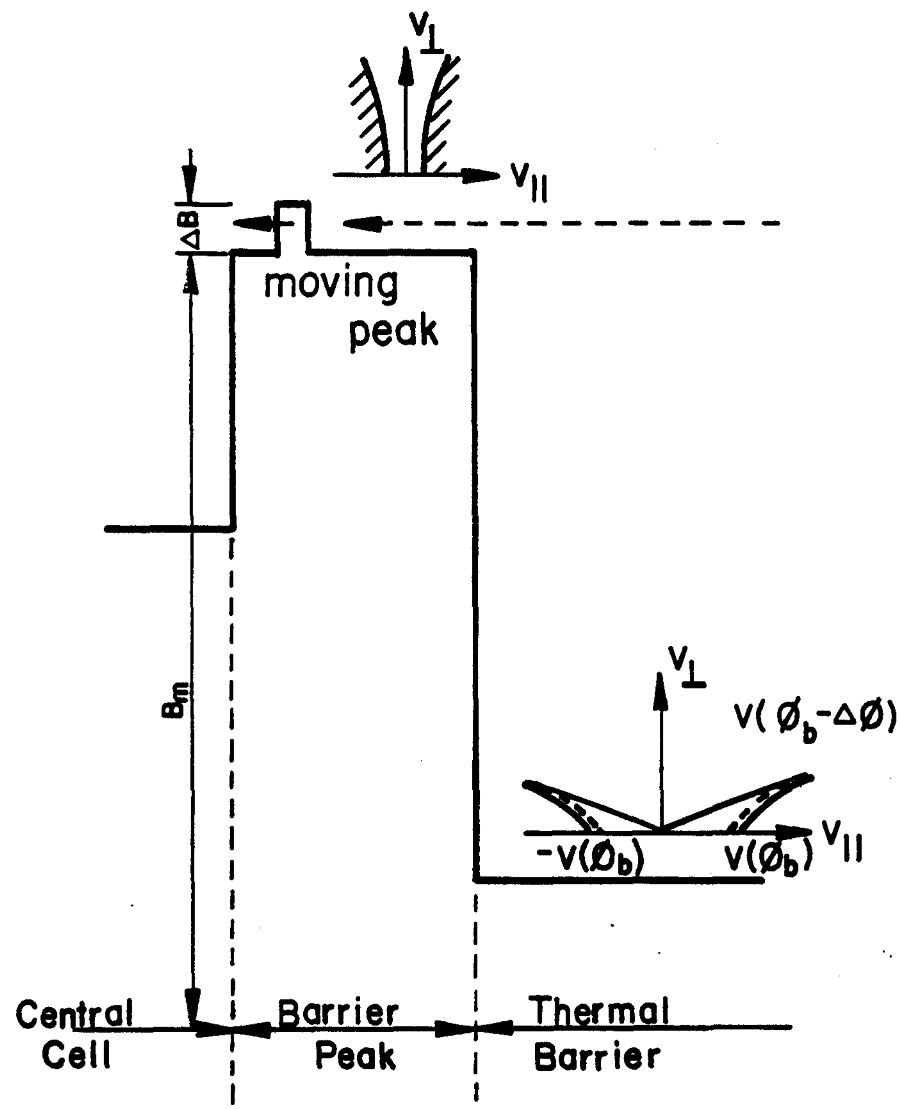

$V_\perp$
$V_{||}$
ΔB
moving peak
B_m
$V_\perp$
$V(\emptyset_b-\Delta\emptyset)$
$-V(\emptyset_b)$
$V(\emptyset_b)$
$V_{||}$
Central Cell
Barrier Peak
Thermal Barrier

FIG. 2a

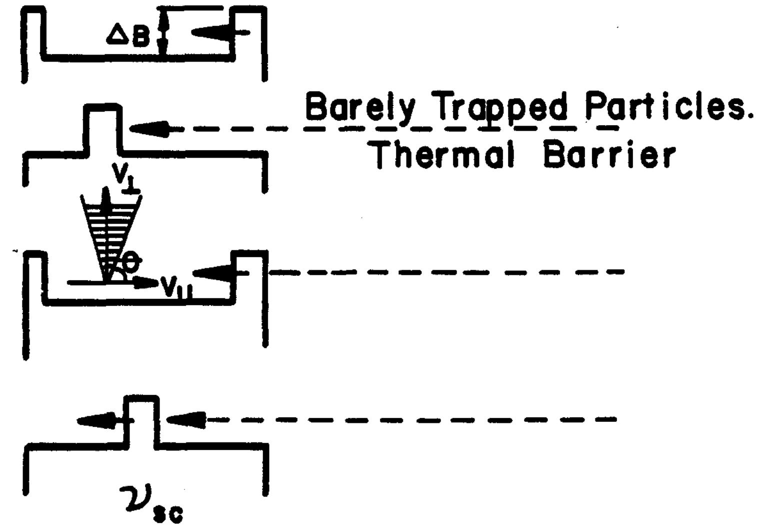

ΔB
Barely Trapped Particles.
Thermal Barrier
$V_\perp$
θ
$V_{||}$
ν_{sc}

FIG. 2b

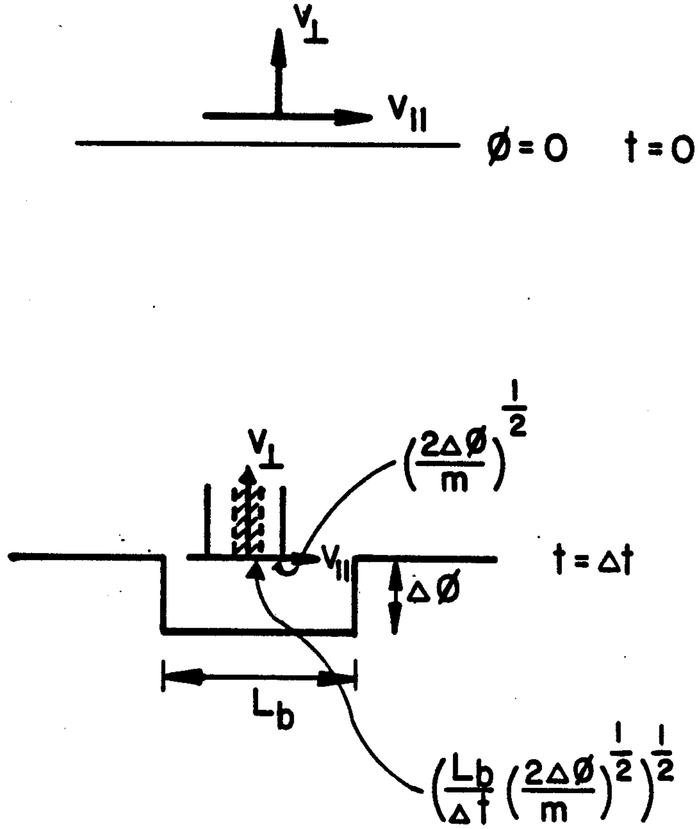

$V_\perp$
$V_{||}$
$\emptyset = 0 \quad t = 0$
$V_\perp$
$\left(\frac{2\Delta\emptyset}{m}\right)^{\frac{1}{2}}$
$V_{||}$
$t = \Delta t$
$\Delta\emptyset$
L_b
$\left(\frac{L_b}{\Delta t}\left(\frac{2\Delta\emptyset}{m}\right)^{\frac{1}{2}}\right)^{\frac{1}{2}}$

FIG. 3

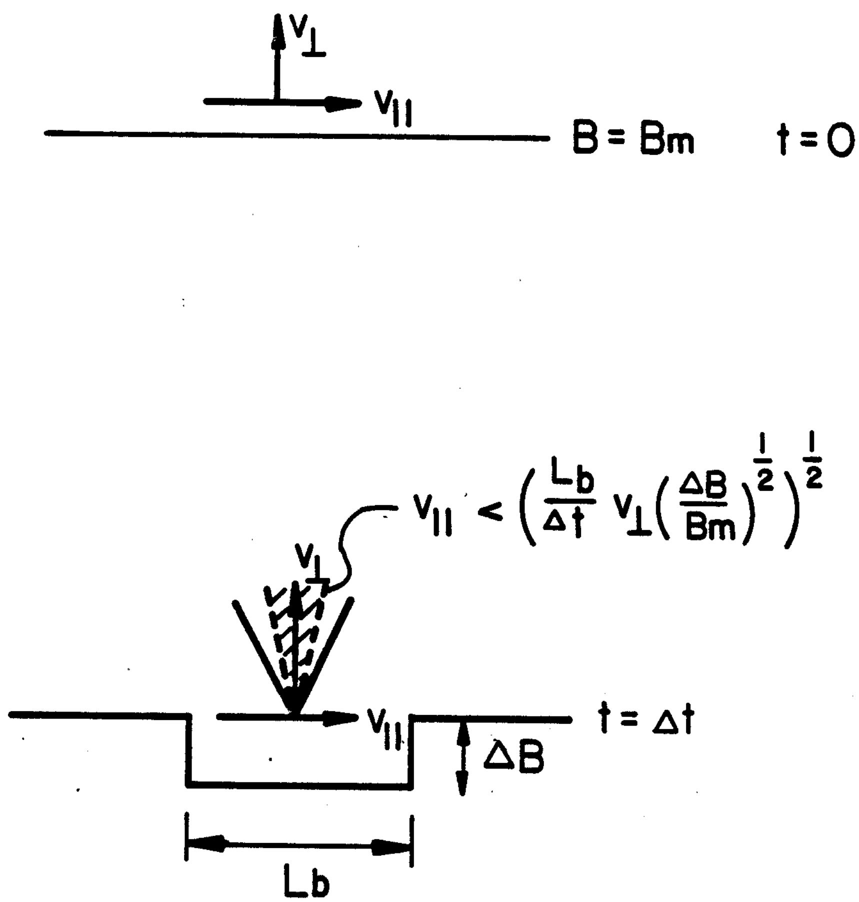

FIG. 4

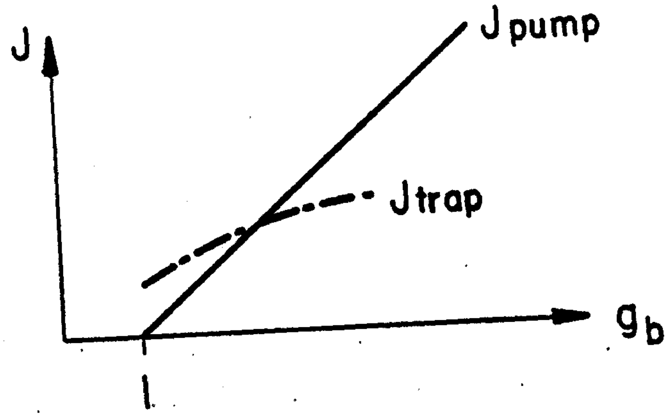

FIG. 5

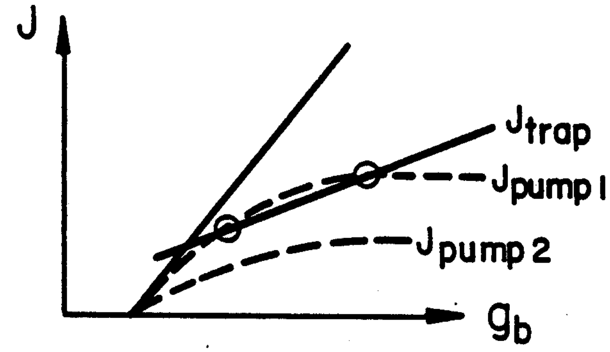

FIG. 6

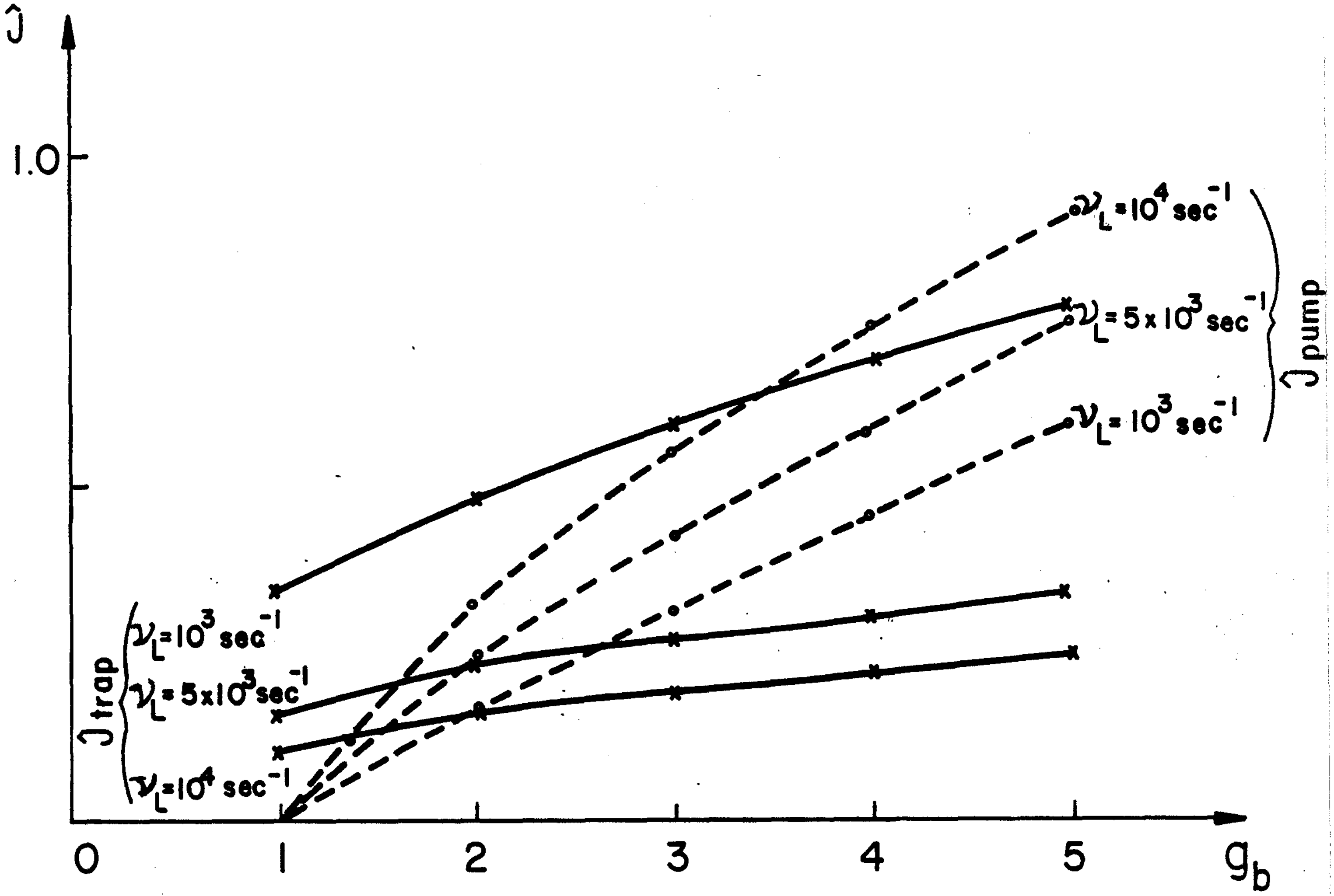

J
1.0
$\nu_L = 10^4 \sec^{-1}$
$\nu_L = 5\times10^3 \sec^{-1}$
$\nu_L = 10^3 \sec^{-1}$
J_{pump}
J_{trap}
$\nu_L = 10^3 \sec^{-1}$
$\nu_L = 5\times10^3 \sec^{-1}$
$\nu_L = 10^4 \sec^{-1}$
0
1
2
3
4
5
g_b

FIG. 7

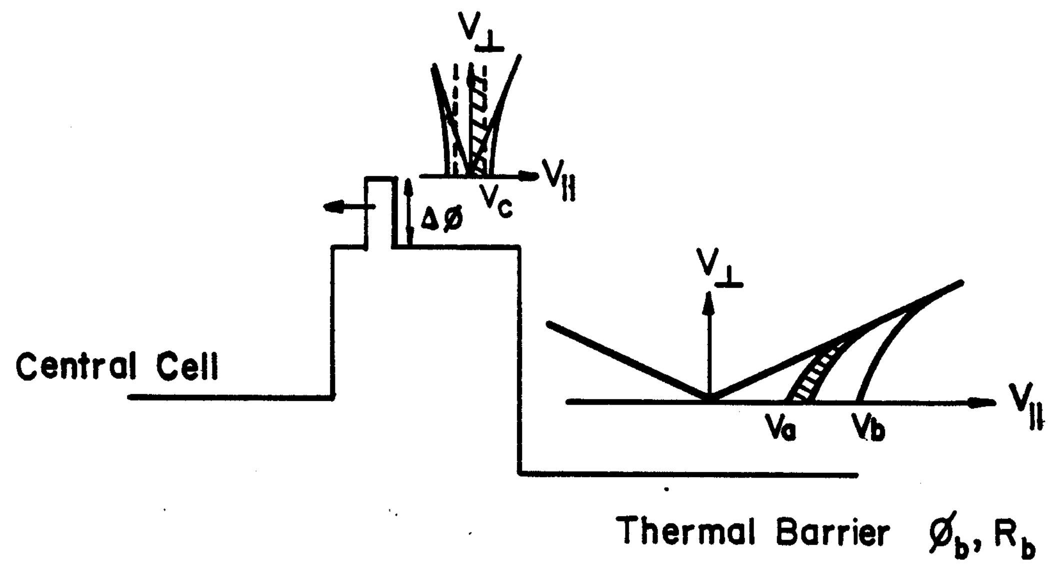

$V_\perp$
$V_\parallel$
V_c
$\Delta\phi$
Central Cell
$V_\perp$
$V_\parallel$
V_a
V_b
Thermal Barrier ϕ_b, R_b

FIG. 8

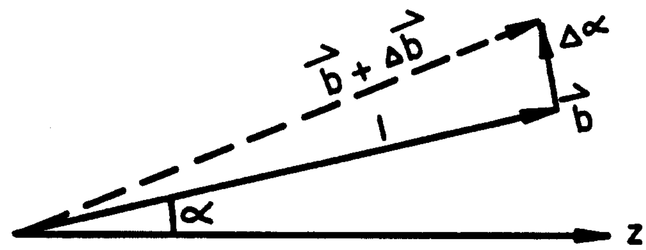

FIG. 8 The derivative of angle α in the normal direction.

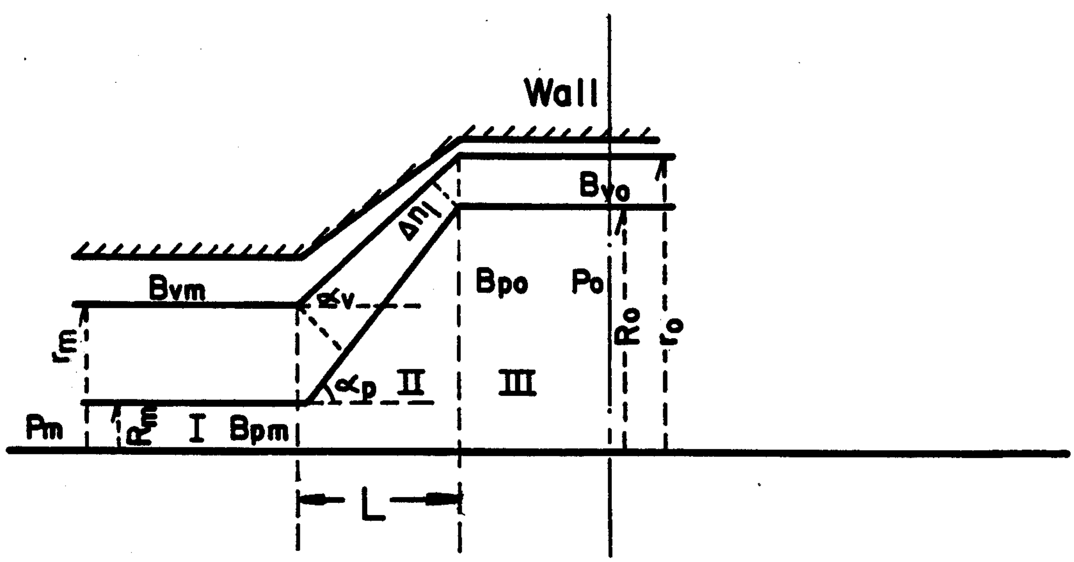

FIG. 9 A straight field line model for non-long-thin case.